

Quasiparticle Scattering Interference in High Temperature Superconductors

Qiang-Hua Wang^{a,b}, and Dung-Hai Lee^a

(a) Department of Physics, University of California at Berkeley, Berkeley, CA 94720, USA

(b) National Laboratory of Solid State Microstructures,

Institute for Solid State Physics, Nanjing University, Nanjing 210093, China

By performing explicit T-matrix calculations we show that scattering by impurities can produce quasiparticle interference patterns recently observed by high resolution scan tunnelling microscopy image of the local density of states in $Bi_2Sr_2CaCu_2O_{8+\delta}$ [5]. This result clarifies the extent by which real-space STM images can extract quasiparticle dispersion in the momentum space.

74.25.Jb,74.25.-q,74.20.-z

Scanning tunnelling microscopy (STM) is a real-space probe of the electron local density of states (LDOS) with atomic resolution. This technique has provided invaluable information on the nature of quasi-particle states in high temperature superconductors [1].

Recently the existence of a competing order parameter becomes the focus of a number of STM studies. For example by applying a magnetic field Hoffman *et al* observed a four-lattice-constant checkerboard LDOS modulation in the LDOS around the cores of superconducting vortices [2]. This modulation occurs in the $(0, \pm 1)$ and $(\pm 1, 0)$ crystalline directions and in the energy range $0 \leq E \leq 12$ meV. Very recently Howald *et al* reported similar modulation at energy $E = 25$ meV but in zero magnetic field [3]. These results have stimulated considerable interests in whether or not an incommensurate charge density wave order exists in $Bi_2Sr_2CaCu_2O_{8+\delta}$ [4].

Recently one of us (DHL) proposed an alternative explanation for the observed LDOS modulation, namely they are the quantum interference patterns of the quasi-particle wave functions after each being scattered by impurities [5]. This proposal is recently tested by Hoffman *et al* using very high resolution LDOS images in samples ranging from under to overdoping [5]. The results show that in zero magnetic field the patterns of LDOS modulation are actually energy dependent. In particular after Fourier transforming the LDOS patterns Hoffman *et al* find two discernible groups of ordering wave vectors. The first is in the $(0, \pm 1)$ and $(\pm 1, 0)$ directions and the second is in the $(\pm 1, \pm 1)$ directions. The wave vectors \mathbf{q} of the first group disperses with energy in such a way that $|\mathbf{q}|$ decreases when the energy increases. On the contrary the wave vectors in the second group increase their length as the energy increases. In addition the dispersion of these two group of wavevectors show systematic but opposite doping dependence. In Ref. [5] Hoffman *et al* identified these wave vectors with elastic scattering processes from one point of the normal state Fermi surface to another and obtained a reasonable agreement with the quasiparticle dispersion found by the angle-resolved photoemission experiment [6,7].

While intuitively appealing, the above identification is only qualitative. It is thus important to carry out an explicit calculation to check the validity of the scattering interference idea [8]. In this paper we report such a calculation and clarify the extent by which the scattering processes postulated by Hoffman *et al* should be observable as features in the local density of states.

We begin by briefly reviewing the quasiparticle scattering interference in a simple metal. Due to translation symmetry the LDOS in an uniform system is invariant under lattice translation. In the presence of impurities the electronic eigen states having the same energy but associated with different wave-vectors can be mixed. This gives rise to a spatial modulation of the amplitude of the scattering wave function, and therefore the LDOS at that particular energy.

To be more specific, let us consider the problem of a single impurity in a simple 3D metal. If we define the position of the impurity to be the origin of the coordinate, the local Green's function $G(i, i, \omega)$ at site i (the quantity necessary to calculate the LDOS) is given by,

$$G(i, i; \omega) = G_0(i, i; \omega) + G_0(i, 0; \omega)T(\omega)G_0(0, i; \omega). \quad (1)$$

Here ω is the energy of interest, G_0 is the Green's function in the absence of impurity, and $T^{-1}(\omega) = V^{-1} - G_0(0, 0; \omega)$ where V is the perturbing potential exerted by the impurity. Since $G_0(i, i; \omega)$ is independent of i , all spatial dependence of $G(i, i; \omega)$ comes from $G_0(i, 0; \omega)$ and $G_0(0, i; \omega)$ in the second term of Eq. (1). The "unperturbed" Greens function $G_0(i, 0, \omega)$ is given by,

$$G_0(i, 0; \omega) = \int \frac{d^3 \mathbf{k}}{(2\pi)^3} \frac{\exp(i\mathbf{k} \cdot \mathbf{r}_i)}{\omega - E_k + i\delta}. \quad (2)$$

For simple dispersion $E_k = k^2/2m - \mu$ it is straightforward to show that

$$G_0(i, 0; \omega) \propto \frac{e^{ik_\omega r_i}}{r_i}, \quad (3)$$

where $k_\omega = \sqrt{2m(\omega + \mu)}$. (In a lattice model r_i has a lower cutoff of one lattice constant.) Due to Eq. (3) the LDOS given by $-ImG(i, i; \omega)/\pi$ will show a spatial modulation with an energy-dependent characteristic wavelength π/k_ω .

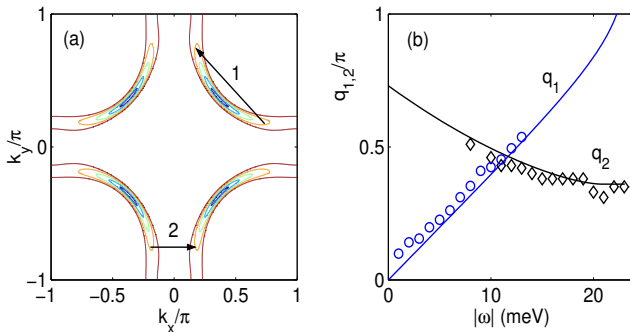


FIG. 1. (a) Schematic plot of banana-shaped equal-energy contours. Contours at higher energies are not shown. The tips of the bananas traces the normal state Fermi surface. The arrows indicate important elastic scattering processes discussed in the text. (b) The energy dependence of the modulation wave vector $q_{1,2}$ associated with the scattering processes 1 and 2 indicated in (a). The solid lines are naive expectations, and the symbols are extracted from the negative bias pictures of Fig. 2(a). A symbol is put down for a particular energy only when there is a discernable peak in the wave vector space. It is interesting to note that only in a narrow energy range peaks in both direction coexist.

In a realistic metal there are other factors limiting the observation of the energy-dependent LDOS modulation. For example, the quasi-particle lifetime gets shorter and shorter for energies away from the Fermi level. As a result the LDOS modulation decays very fast away from the location of the impurity. Even with very sharply defined quasiparticle the large band width of normal metals makes the change of k_ω in the energy range of a few meV very difficult to detect.

In the normal state the Fermi surface of Bi-2212 consists of four hole-like Fermi arcs. [6] The quasiparticles are however, poorly defined. In the superconducting state a d-wave gap opens up, and at the same time quasiparticles become well-defined [7]. In the following we assume ideal Bogoliubov quasiparticles and calculate the effect of scattering interference on their LDOS. First let us understand the equal-energy contours (EEC) for the quasiparticle dispersion. Since experimentally LDOS modulation is only observed for energies lower than the maximal gap, we shall concentrate on that energy range here. Around each of the four gap node the EEC evolves from a single point at zero energy, to banana-shaped closed contours at higher energies. The size of the banana increases with the energy until its tips touch the Brillouin zone. When that happen the EEC changes from closed to open contours. This is schematically shown in Fig.1, where differently colored EEC's represent different quasiparticle energies.

Due to the large difference between v_F and v_Δ ($v_F/v_\Delta \approx 20$ at the gap nodes, here v_F is the normal state Fermi velocity, and v_Δ is the tangential derivative of the superconducting gap along the Fermi surface)

the EEC moves with energy the fastest at the tips of the banana. As a result scattering processes connecting the tips have a significantly larger joint density of states. This qualitative argument leads to the prediction that the most prominent LDOS modulation wave vectors should be the set of all possible vectors connecting pairs of banana tips. Out of the seven possible vectors, two of them are indicated by numbered arrows 1-2 in Fig. 1. Knowing the value of quasiparticle energy at the energy of the tips of the banana allows us to predict the energy dependence of these wave-vectors, and this is shown as the solid lines in Fig.1(b).

The above expectations based on the joint density of state are qualitative. The result of an exact scattering calculation using Eq. (1) can differ from the above expectation due to the following complications. 1) The effect of coherence factor: the scattering matrix element between quasiparticle states at momentum k and k' by scalar and/or magnetic impurities is proportional to $(V_m + V_s)u_k u_{k'} + (V_m - V_s)v_k v_{k'}$, with

$$u_k = \pm \text{sgn}(\Delta_k) \sqrt{(1 \pm \epsilon_k/E_k)/2},$$

$$v_k = \sqrt{(1 \mp \epsilon_k/E_k)/2}.$$

In the above the upper/lower sign applies for positive/negative energy quasiparticle states, ϵ_k is the normal state dispersion, Δ_k is the gap function, and $E_k = \sqrt{\epsilon_k^2 + \Delta_k^2}$. In addition V_s (V_m) is the strength of the scalar (magnetic) scattering. For d-wave pairing Δ_k changes sign in processes 1. Therefore depending on whether the scattering process is scalar or magnetic in nature, processes 2 or 1 will be relatively suppressed. 2) The “off-shell” contributions: the above joint density of state picture is based on approximating the G_0 ’s in Eq. (3) by their imaginary part. In reality the real part of G_0 also contributes. These contributions arise from off-shell process which act to blur the modulation wave vectors predicted by the joint density of states argument. In the following we perform an explicit calculation to see the extent by which the joint density of state picture gives the right answer.

For the quasiparticle Hamiltonian, we use a model provided by Norman *et al.* [9] To be explicit

$$H = \sum_{k\sigma} \epsilon_k C_{k\sigma}^\dagger C_{k\sigma} - \sum_k (\Delta_k C_{k\uparrow} C_{-k\downarrow} + \text{h.c.}). \quad (4)$$

In the above $\epsilon_k = \sum_{n=0}^5 t_n \chi_n(k)$ and $\Delta_k = \Delta_0 (\cos k_x - \cos k_y)/2$, where $t_{0-5} = 0.1305, -0.5951, 0.1636, -0.0519, -0.1117, 0.0510$ (eV), and $\Delta_0 = 0.025$ eV. Moreover $\chi_{0-5}(k) = 1, (\cos k_x + \cos k_y)/2, \cos k_x \cos k_y, (\cos 2k_x + \cos 2k_y)/2, (\cos 2k_x \cos k_y + \cos 2k_y \cos k_x)/2$, and $\cos 2k_x \cos 2k_y$.

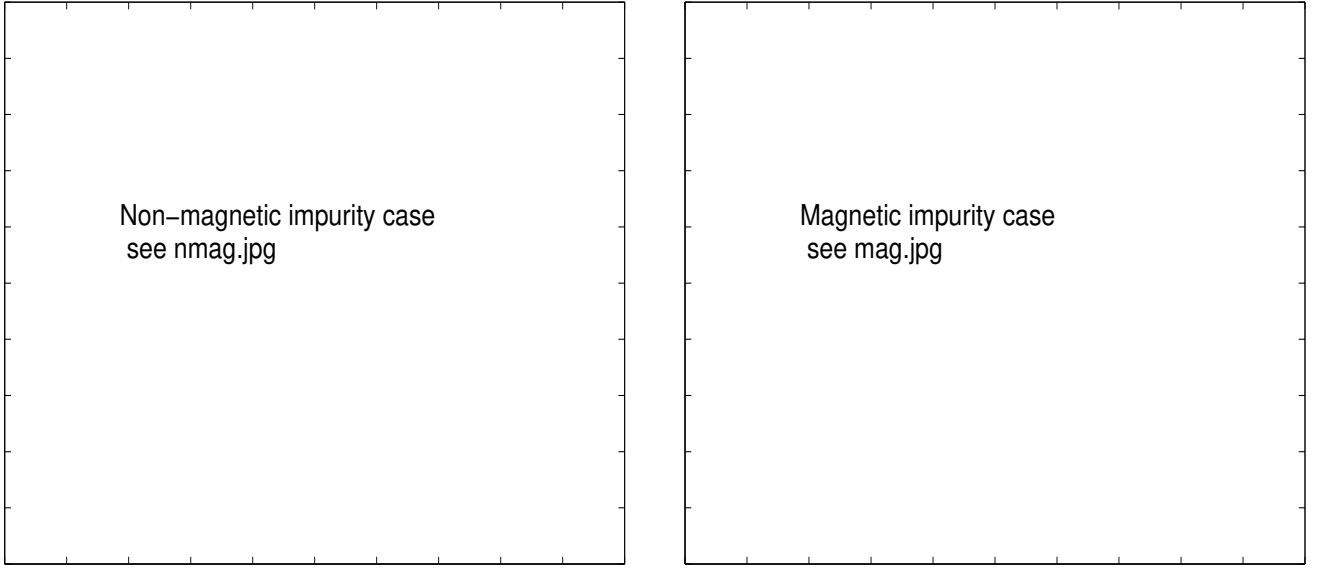


FIG. 2. Fourier amplitudes of the LDOS maps at the given energies as a function of momenta in the first Brillouin zone for (a) $(V_s, V_m) = (100\text{meV}, 0)$ and (b) $(V_s, V_m) = (0, 100\text{meV})$. The numbers on the sub-graphs show the energy in units of meV. The hot/cold color denotes higher/lower strength. **The eps and jpg files for this figure, namely, nmag.jpg and mag.jpg, can be found in the source file package.**

In a superconductor a quasiparticle has electron and hole components. As a result the quantities in Eq. (1) become 2×2 matrices. In particular

$$G_0(i, 0; \omega) = \int \frac{d^2\mathbf{k}}{(2\pi)^2} \frac{\omega I + \epsilon_k \sigma_3 + \Delta_k \sigma_1}{(\omega + i\delta)^2 - E_k^2} e^{i\mathbf{k} \cdot \mathbf{r}_i}, \quad (5)$$

and

$$T^{-1}(\omega) = (V_s \sigma_3 + V_m I)^{-1} - G_0(0, 0; \omega). \quad (6)$$

The LDOS is given by

$$\rho(i; \omega) = -\frac{1}{\pi} \text{Im}[G_{11}(i, i; \omega) + G_{22}(i, i; -\omega)]. \quad (7)$$

In order to accurately take into account the contribution to G_0 from the thin bananas in Fig.1(a), a momentum resolution $\delta k \ll \pi v_\Delta / v_F$ must be achieved. This in turn means that a large real space lattice has to be used for the actual calculation. For the results reported below a 400×400 lattice is used. In this calculation we did not take the self-consistent suppression of the pairing amplitude near the impurity into account. However we do not expect this omission to cause any significant change because the impurity scattering strength we used is much larger than the maximal pairing gap. [10]

In the following two kinds of impurities are studied: (a) non-magnetic impurity ($V_s = 100\text{meV}$ and $V_m = 0$) and (b) magnetic impurity ($V_s = 0$ and $V_m = 100\text{meV}$). By using two extreme types of scatterer we can study the dependence of the quasiparticle interference pattern on the nature of scattering processes. The impurity strength we choose is moderately weak in the sense that we do not

see quasiparticle resonance states in the LDOS. [11] (Resonant states appear above $V_{s,m} \sim 1\text{eV}$.) The reasons we choose this kind of non-unitary scatterer are two folds: 1) They are not easily identifiable via quasiparticle resonance in LDOS. (In the experimental case, no resonant states are present in the given view field. [5]) 2) They turn out to have a stronger effect on the quasiparticle interference than the unitary scatterers.

Figs.2 shows the Fourier amplitude of the LDOS maps at $\omega = -24 \rightarrow -3 \text{ meV}$ and $\omega = 3 \rightarrow 24 \text{ meV}$ with 3 meV interval for (a) nonmagnetic, and (b) magnetic impurity. In these figures the intensity at $\mathbf{q} = 0$ is subtracted so that weaker features at other wave vectors can show up. In constructing Figure 2 the LDOS of the central 51×51 plaquette in the 400×400 lattice are Fourier transformed. It is interesting to note that in real experiment a large field of view is also employed in the Fourier transform in order to achieve high momentum resolution.

For the negative energies in Fig.2(a) the Fourier peaks in the $(\pm 1, \pm 1)$ direction is clearly visible between -3 to -12 meV . Moreover as the binding energy increases the peaks moves away from the origin. For binding energy 18 meV and above the Fourier peaks in the $(0, \pm 1)$ and $(\pm 1, 0)$ appear. Contrary to the diagonal direction spots these peaks move only slightly as the energy varies. Careful analysis of such movement indicates that these peaks move toward the origin as the binding energy increases. The energy dependence of the these LDOS Fourier peaks is shown in Figure 1(b) as symbols. The difference between the naive expectation (solid lines) and the results of T-matrix calculation (symbols) is very small. This comparison clarifies the extent by which the qualitative

picture of joint density of states works. It is interesting to note that a significantly bigger deviation exists between the observed LDOS modulation wave vectors and those expected from angle-resolved photoemission data [5]. In addition to the above peaks there are other weaker features in Fig.2(a). These features can either be identified as the higher harmonics of the diagonal and vertical/horizontal spots or can be attributed to the other scattering processes not shown in Fig.1 [12]. The diagonal direction quasiparticle interference patterns are sensitive to the sign of the bias voltage. We find the diagonal Fourier peaks become much weaker at positive energies in Fig.2(a). On the contrary the $(0, \pm 1)$ and $(\pm 1, 0)$ direction peaks seem to be insensitive to the bias reversal.

We have investigated the issue of plus/minus bias voltage asymmetry of the $(\pm 1, \pm 1)$ direction Fourier peaks further. We find the detailed quasiparticle dispersion has important effects on this asymmetry. For example by setting all the t_n except $n = 1$ to zero we find the asymmetry disappears. Therefore we conclude that we can not make a definitive prediction of the bias asymmetry.

The quasiparticle interference patterns for magnetic impurity in Fig.2(b) are quite different from those shown in Fig.2(a). For example the amplitude of the $(\pm 1, \pm 1)$ direction modulation for $|\omega| \leq 12$ meV is much weaker. The fact that the $(\pm 1, \pm 1)$ direction peaks are weaker than the $(\pm 1, 0)$ and $(0, \pm 1)$ direction peaks is consistent with the coherence factor effect discussed previously.

In addition to the above differences there are similarities between Figs. 2(a) and 2(b). For example at $|\omega| = 21, 24$ meV, the patterns in (a) and (b) become rather similar. In the same energy range the asymmetry between positive and negative bias becomes small. In this energy range the horizontal component of the scattering wavevector associated with process 2 cease to change with energy. As the result the modulation wave-vectors in the $(\pm 1, 0)$ and $(0, \pm 1)$ directions hardly change.

Upon closing a few remarks are in order. First, the present result demonstrates that quasiparticle interference due to scattering by scalar (non-unitary) impurities can produce LDOS modulation similar to that observed in recent STM experiment [5]. This effect reflects single quasiparticle quantum mechanics and has nothing to do with the presence of a charge density wave order. Whether a very weak LDOS modulation due to charge density wave order is hidden under the quasiparticle interference pattern has to be answered by future experiments. Second, the results of the present paper requires sharply defined quasiparticles. In particular the quasiparticle energy broadening is taken to be 1 meV in this paper. Upon using larger broadening we find the intensity of the $(\pm 1, \pm 1)$ direction modulation diminishes. In contrast the $(\pm 1, 0)$, $(0, \pm 1)$ direction modulation is robust. Whether well-defined quasiparticle is a necessary condition for observing LDOS modulations is currently under investigation [13]. Third, the present paper

only addresses the quasiparticle interference caused by the scattering of a single impurity. In the presence of many impurities how are the interference patterns from different impurities patched together needs to be further studied. Forth, whether the existence of quasiparticle interference is consistent with a substantial gap modulation in the CuO_2 plane should be investigated further. Finally what is the relation between the relatively weak quasiparticle interference observed at zero magnetic field [5] and the relatively strong checkerboard LDOS modulation near superconducting vortices [2] is currently unclear.

ACKNOWLEDGMENTS

This work is supported by DMR 99-71503. QHW is also supported by the Natural Science Foundation of China, and the Grant for State Key Program of China grant No. G1998061407. We thank J.C. Davis's group at Berkeley for sharing their unpublished data with us. We are also grateful for the helpful discussions with J.C. Davis, M. E. Flatte, Jung Hoon Han, J.E. Hoffman, S. A. Kivelson, K. McElroy, J. Orenstein, Z. X. Shen and R. W. Simmonds.

- [1] See, *e.g.*, E. W. Hudson, *et al*, *Science* **285**, 88 (1999); A. Yazdani, *et al*, *Phys. Rev. Lett.* **83**, 176 (1999); S. H. Pan, *et al*, *Nature* **403**, 746 (2000); E. W. Hudson, *et al*, *Nature* **411**, 920 (2001); K. M. Lang, *et al*, *Nature* **415**, 412 (2002).
- [2] J. Hoffman, *et al*, *Science* **295**, 466 (2002).
- [3] C. Howald, H. Eisaki, N. Kaneko, and A. Kapitulnik, cond-mat/0201546.
- [4] See, *e.g.*, S. Sachdev, cond-mat/0203363 (and references cited therein); M. Vojta, cond-mat/0204284; Han-Dong Chen, *et al*, cond-mat/0203332; Jian-Xin Zhu, Ivar Martin, and A. R. Bishop, cond-mat/0201519; M. Franz, D. E. Sheehy, and Z. Tesanovic, cond-mat/0203219.
- [5] J. Hoffman *et al*, submitted to *Science*.
- [6] For a review of the angle-resolved-photo-emission study of the electronic structure in the cuprates, see, *e.g.*, A. Damascelli, D.H. Lu, Z.-X. Shen, *J. Electron Spectr. Relat. Phenom.* **117-118**, 165 (2001) (cond-mat/0107042), and references cited therein.
- [7] D. L. Feng, *et al*, *Science* **289**, 277 (2000).
- [8] For an earlier proposal of detecting the anisotropic quasiparticle scattering interference in d-wave superconductor see J.M. Byers, M.E. Flatte and D.J. Scalapino, *Phys. Rev. Lett.* **71**, 3363 (1993); J.M. Byers and M.E. Flatte *Phys. Rev. Lett.* **80**, 4546 (1998).
- [9] M. R. Norman, M. Randeria, H. Ding and J. C. Campuzano, *Phys. Rev. B* **52**, 615 (1994).

- [10] Some effects of gap suppression by a point impurity can be found in, *e.g.*, A. Shnirman, I. Adegideli, P. M. Goldbart, and A. Yazdani, Phys. Rev. B **60**, 7517 (1999); M. H. Hettler, and P. J. Hirschfeld, Phys. Rev. B **59**, 9606 (1999).
- [11] A. V. Balatsky, M. I. Salkola, and A. Rosengren, Phys. Rev. B **51**, 15547 (1995); M. I. Salkola, A. V. Balatsky, and D. J. Scalapino, Phys. Rev. Lett. **77**, 1841 (1996).
- [12] R. W. Simmonds and J.C. Davis, private communication; K. McElroy *et al.*, to be published.
- [13] S.A. Kivelson, private communication.

This figure "mag.jpg" is available in "jpg" format from:

<http://arxiv.org/ps/cond-mat/0205118v1>

This figure "nmag.jpg" is available in "jpg" format from:

<http://arxiv.org/ps/cond-mat/0205118v1>